

# Theoretical Study of the Role of the Funny Current ( $I_f$ ) and the Background Inward Current ( $I_b$ ) in Atrioventricular Nodal Conduction

Jue Li, Ian Temple, Mark Boyett

Institute of Cardiovascular Sciences, University of Manchester, UK

## Abstract

The aim of the study is to theoretically explore the role of  $I_f$  in atrioventricular nodal conduction using computer simulation. The background current,  $I_b$ , is another inward current flowing during diastole and this was also investigated. We began with Inada's model of the rabbit atrioventricular nodal action potential (N-type). There is uncertainty from experiments about the magnitude and properties of  $I_f$ . Therefore, the properties of  $I_f$  and  $I_b$  in the model were varied. Four different cases were analysed. A one-dimensional model made up of 100 elements, each 100  $\mu\text{m}$  in length, was used. The diffusion coefficient,  $D$ , was set to 0.001  $\mu\text{S mm}^2$ . One end of the string (elements 1 to 3) was stimulated at 3 Hz. The conduction velocity was calculated from the times of arrival of the action potential at the 41th and 61th elements. In Inada's original model, blocking  $I_f$  resulted in a 0.85% slowing of conduction, whereas blocking  $I_f$  in a modified model had a greater effect (19.4% slowing in Case 4). The results show that  $I_f$  can theoretically influence the conduction velocity of the atrioventricular node.

## 1. Introduction

The conduction system in the heart initiates and transmits electrical signals (action potentials), which coordinate the heart contraction. There are three main parts of the cardiac conduction system – the sinoatrial node (SAN), atrioventricular node (AVN) and His-Purkinje system. The AVN lies within the triangle of Koch bounded by the coronary sinus, tendon of Todaro, and tricuspid valve. The AVN is the only site where the action potential can pass from the atria to the ventricles.

$I_f$  (hyperpolarization-activated current) is an inward current flowing during diastole. It is an important pacemaker current in the SAN, but it is also present in the AVN. The role of  $I_f$  in generation of spontaneous activity is well established [1]. HCN (hyperpolarization-activated cyclic nucleotide-gated) channels are responsible for  $I_f$ . HCN channels are encoded by four genes (HCN 1~4).

HCN4 is the main isoform expressed in the cardiac conduction system.

Surprisingly, there is functional evidence that  $I_f$  affects AVN conduction. Although ivabradine has not been shown to have an effect on the human AVN, another  $I_f$  blocking agent, zatebradine, has been shown to increase the AH interval, atrioventricular node effective refractory period, and Wenckebach cycle length in humans[2]. Ivabradine has also been shown to slow the ventricular response to atrial fibrillation in dogs with the mechanism thought to be the result of specific block of  $I_f$  within the AVN slowing conduction[3]. Finally, inducible cardiac specific knockout of HCN4 in mice is lethal due to the development of complete heart block (complete block of AVN conduction)[4]. This is of interest, because there is heart block (slowing of AVN conduction) in pulmonary hypertension and we have observed a downregulation of HCN4 in the AVN in a rat model of pulmonary hypertension[5].

This paper aims to theoretically explore the role of  $I_f$  in AVN conduction using computer simulation. A model of the rabbit AVN action potential (N-type) [6] was first modified to replicate the role of  $I_f$  in the spontaneous activity of the AVN. A one-dimensional model made up of 100 elements, each 100  $\mu\text{m}$  in length, was used.

## 2. Methods

To simulate the AVN action potential, the model of the rabbit AVN action potential (N-type) from Inada *et al.* [6] was used. General equations are:

$$\frac{dV}{dt} = -\frac{I_{total}}{C_m} \quad (1)$$

$$I_{total} = I_{Ca,L} + I_{K,r} + I_f + I_{st} + I_p + I_{NaCa} + I_b \quad (2)$$

where  $V$  (mV) is the membrane potential,  $t$  (ms) is the time,  $I_{total}$  (pA) is the total membrane current, and  $C_m$  (pF) is the membrane capacitance. The total membrane current is the sum of seven ionic currents, which are shown in

equation (2). A one-dimensional model was used to simulate conduction in the AVN. The model includes 100 elements and each element is 100  $\mu\text{m}$  in length. The reaction-diffusion equation was used:

$$\frac{\partial V}{\partial t} = -\frac{I_{total}}{C_m} + D \frac{\partial^2 V}{\partial x^2} \quad (3)$$

where  $D$  is the diffusion coefficient.

## 2.1. Modification of the AVN model to improve the spontaneous rate control by $I_f$

The role of  $I_f$  in spontaneous rate control is well established [1,4,7]. Results from Baruscotti *et al.* [4] from a cardiac-specific HCN4 knockout mouse model revealed a strong reduction of both  $I_f$  (by  $\sim 70\%$ ) and the spontaneous rate (by  $\sim 60\%$ ) in the SAN. In the Liu *et al.* [7] reported that blocking  $I_f$  increased the spontaneous cycle length in both the SAN (by  $\sim 12.85\%$ ) and AVN (by  $\sim 73.56\%$ ).

Using the original AVN (N-type) model from Inada *et al.* [6], block of  $I_f$  increased the spontaneous cycle length from 463 ms to 471 ms ( $\sim 2\%$  increase). The increase was much less than in experiments. In the Inada *et al.* [6] model, it is possible that  $I_f$  has been underestimated due to the lack of experimental data. There is uncertainty from experiments about the magnitude and properties of  $I_f$ . Therefore, it is reasonable to modify  $I_f$ .  $I_b$  is another inward current flowing during diastole. In the original AVN (N-type) model from Inada *et al.* [6], the conductance and equilibrium potential of  $I_b$  was adjusted to obtain a reasonable resting potential [6]. Figure 1 shows  $I_f$  and  $I_b$  currents in the original AVN (N-type) model from Inada *et al.* [6].  $I_f$  is much smaller than  $I_b$ .

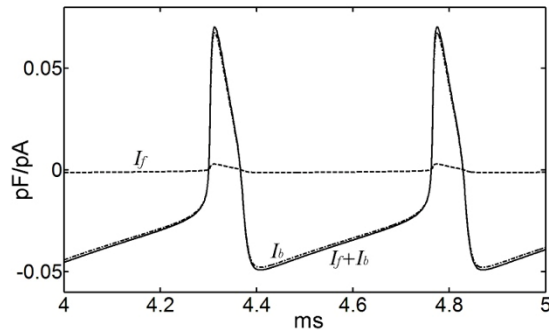


Figure 1.  $I_f$ ,  $I_b$  and sum of both currents in the original AVN (N-type) model from Inada *et al.* [3].

To obtain reasonable spontaneous rate control by  $I_f$ ,  $I_f$  and  $I_b$  in the N-type model were modified by increasing  $I_f$  and adjusting  $I_b$  at the same time to obtain the same action potential shape and the same spontaneous cycle length. The equations for  $I_f$  and  $I_b$  are:

$$y_\infty = \frac{1.0}{1.0 + \exp((V - V_{1/2})/k)}$$

$$\tau_y = 0.25 + 2.0 \exp(-(V - (-70))^2 / 500) \quad (4)$$

$$\frac{dy}{dt} = \frac{y_\infty - y}{\tau_y}$$

$$I_f = g_f y (V - E_f)$$

$$I_b = g_b (V - E_b) \quad (5)$$

where  $y$  is the activation variable of  $I_f$ ,  $y_\infty$  is the voltage-dependent steady-state value of  $y$ ,  $\tau_y$  is the voltage-dependent time constant of  $y$ ,  $V_{1/2}$  is the voltage at which half activation occurs, and  $k$  is a factor determining how steeply the activation curve changes with voltage.  $g_f$  and  $g_b$  are the conductances for  $I_f$  and  $I_b$ , respectively.  $E_f$  and  $E_b$  are the equilibrium potentials of  $I_f$  and  $I_b$ , respectively.

The parameters ( $V_{1/2}$ ,  $k$ ,  $g_f$ ,  $g_b$ ,  $E_f$ ,  $E_b$ ) were chosen to be adjusted. Firstly, the parameters of  $I_f$  were defined. Secondly, the parameters of  $I_b$  were adjusted carefully to achieve the same action potential shape. Four different cases were investigated:

- Case 1: shift the half activation voltage of  $I_f$  by +20 mV and flatten the activation curve of  $I_f$  by increasing  $k$  from 13.56 to 20; adjust the conductance of  $I_b$  to 1.075 nS.
- Case 2: increase the conductance of  $I_f$  by 5 times; adjust the conductance of  $I_b$  to 1.06 nS.
- Case 3: shift the half activation voltage of  $I_f$  by +20 mV and increase the conductance of  $I_f$  by 5 times; adjust the conductance of  $I_b$  to 0.68 nS.
- Case 4: shift the half activation voltage of  $I_f$  by +20 mV, increase the conductance of  $I_f$  by 5 times and shift the equilibrium potential of  $I_f$  by +10 mV; adjust the conductance and equilibrium potential of  $I_b$  to 0.68 nS and -35 mV.

The parameters are summarised in Table 1.

Table 1. Parameters of  $I_f$  and  $I_b$  in Cases 1~4.

	Control	Case 1	Case 2	Case 3	Case 4
$V_{1/2}$ (mV)	-83.19	-83.19	-83.19	-83.19	-83.19
		+20		+20	+20
$k$	13.56	20	13.56	13.56	13.56
$g_f$ (nS)	1	1	5	5	5
$g_b$ (nS)	1.2	1.075	1.06	0.68	0.68
$E_f$ (mV)	-30	-30	-30	-30	-20
$E_b$ (mV)	-22.5	-22.5	-22.5	-22.5	-35

## 2.2. The properties of the action potential in the four cases

Figure 2 shows the  $I_f$  activation curves in the control (original model from Inada *et al.* [6]) and Cases 1~4. The activation curve is not affected by changing the conductance and equilibrium potential of course. Therefore,  $I_f$  in the control and Case 2, and  $I_f$  in Cases 3 and 4, have same activation curve.

Figure 3 shows the action potentials in the control and Cases 1~4. It is not possible to distinguish the five action potentials from each other.

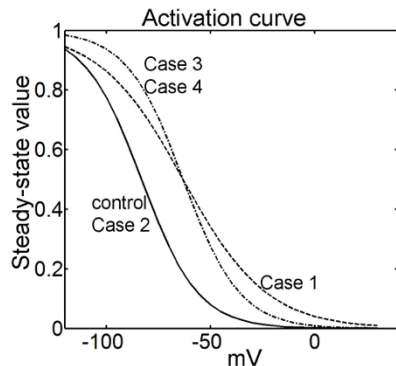


Figure 2. Activation curves of  $I_f$  in the control and Cases 1~4.

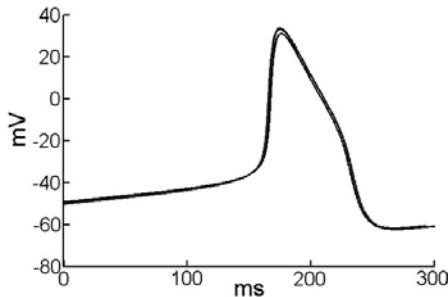


Figure 3. Action potentials in control and Cases 1~4.

Figure 4 shows the time course of  $I_f$  and  $I_b$  in the control and Cases 1~4.  $I_f$  was increased and  $I_b$  decreased in all four cases, particularly in Cases 3 and 4. Table 2 shows the spontaneous cycle length before and after blocking  $I_f$  in the control and the four cases. The spontaneous rate control by  $I_f$  was increased in all cases, particularly in Cases 3 and 4.

Table 2. Spontaneous cycle length (CL) before and after blocking  $I_f$  in control and Cases 1~4.

	CL( $I_f$ )	CL(no $I_f$ )	Changes
Control	462 ms	471 ms	↑2%
Case 1	465 ms	510 ms	↑9.7%
Case 2	463 ms	510 ms	↑10%
Case 3	464 ms	732 ms	↑58%
Case 4	462 ms	∞	∞

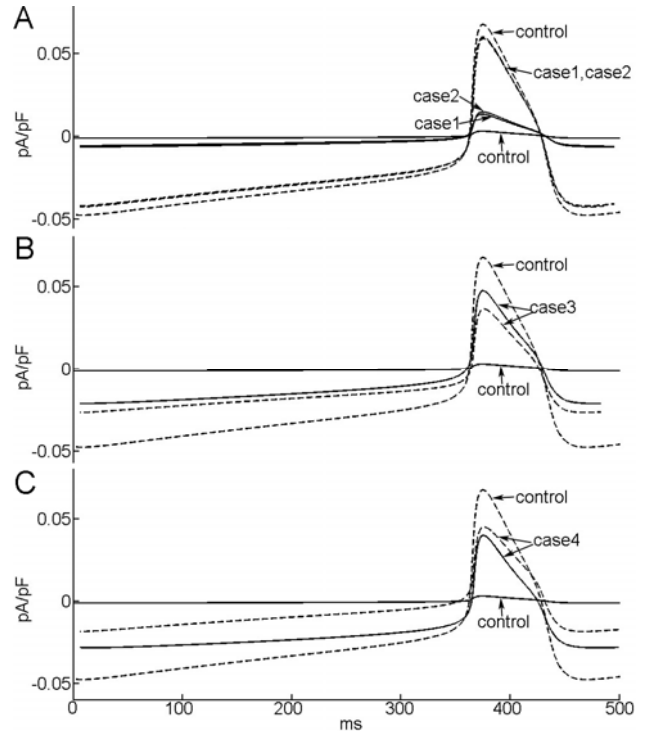


Figure 4. Time course of  $I_f$  (solid line) and  $I_b$  (dashed line) in control and Cases 1 and 2 (A), Case 3 (B) and Case 4 (C).

There were similar changes in Cases 1 and 2.  $I_f$  was increased and  $I_b$  decreased by similar amounts (Figure 4A); the spontaneous cycle length was increased by a maximum of ~10% on blocking  $I_f$  (Table 2). In Case 3, the changes in  $I_f$  and  $I_b$  were greater and now  $I_f > I_b$  (Figure 4B); the spontaneous cycle length was increased by ~58% on blocking  $I_f$  (Table 2). The change in spontaneous cycle length is comparable to that in the mouse AVN [7].

Case 4 was based on Case 3 and a shift of the equilibrium potential of  $I_f$  by +10 mV ( $-30+10= -20$ mV), which agrees with experimental data [8]. The equilibrium potential of  $I_b$  was adjusted accordingly ( $-22.5$  to  $-35$  mV) (Table 1).  $I_f$  shifted inwards (negative direction) and  $I_b$  shifted outwards (positive direction) (Figure 4C). In Case 4, spontaneous activity ceased on blocking 80%  $I_f$ . Figure 5 shows the relationship between the spontaneous cycle length and the percentage of unblocked  $I_f$  in Case 4. It shows that the spontaneous cycle length and the remaining percentage of  $I_f$  are correlated in a negative nonlinear fashion. The spontaneous activity ceased when the percentage of  $I_f$  remaining decreased to 20%.

The above demonstrates that the role of  $I_f$  in spontaneous rate control can be simulated successfully (specifically by Cases 3 and 4; Table 2) without altering the action potential shape.

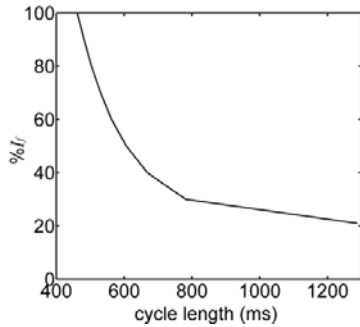


Figure 5. Relationship between the spontaneous cycle length and the percentage of  $I_f$  remaining in Case 4.

### 2.3. Measurement of conduction velocity

To simulate the conduction through the AVN, a one-dimensional model 10 mm in length was used. The model includes 100 elements. One end of the model (elements 1 to 3) was stimulated at 3 Hz. The conduction velocity was calculated from the times of arrival of the action potential at the 41<sup>th</sup> and 61<sup>th</sup> elements to avoid the influence of the boundary (recording point, -20mV during action potential upstroke). The diffusion coefficient,  $D$ , was set to 0.001  $\mu\text{S mm}^2$ .

## 3. Results

Table 3 shows the conduction velocity measured using the one-dimensional model in the control and Cases 1~4. It shows that the conduction velocity was decreased on blocking  $I_f$ . There was a substantial decrease in Cases 3 and 4.

Table 3. The conduction velocity (CV) before and after blocking  $I_f$  in the control and Cases 1~4.

	CV( $I_f$ )	CV(no $I_f$ )	Changes
Control	0.0946 m/s	0.0938 m/s	↓0.85%
Case 1	0.0972 m/s	0.0910 m/s	↓6.4%
Case 2	0.0944 m/s	0.0907 m/s	↓3.9%
Case 3	0.0938 m/s	0.0829 m/s	↓11.6%
Case 4	0.0939 m/s	0.0757 m/s	↓19.4%

## 4. Discussion and conclusion

In this study, we used computer simulation to analyse the role of  $I_f$  in AVN conduction. Firstly, the model of the AVN action potential (N-type) from Inada *et al.* [6] was verified. It was found that the model could not replicate the control of spontaneous rate by  $I_f$  arguably because the density of  $I_f$  was underestimated. It is possible that this is the result of a lack of experimental data. Secondly,  $I_f$  and  $I_b$  in the N-type model from Inada *et al.* [6] were modified to replicate the control of spontaneous rate by  $I_f$  and keep the action potential shape and the spontaneous cycle

length unchanged. Four modified cases were examined. Cases 3 and 4 are the better models in replicating the control of spontaneous rate by  $I_f$  [4, 7]. Finally, the modified models were used in a one-dimensional model to assess the role of  $I_f$  in AVN conduction. The results show that blocking  $I_f$  can lead to a slowing of conduction through the AVN and this is consistent with emerging experimental data[2-4]. It is likely that  $I_f$  controls the excitability of the cell and therefore the conduction velocity. In conclusion, the modelling suggests that  $I_f$  is not only involved in pacemaking - it is also involved in AVN conduction. This raises the possibility that downregulation of HCN4 could slow SAN pacemaking and AVN conduction - this occurs in pulmonary hypertension.

## Acknowledgements

This work is supported by the British Heart Foundation (programme grant, RG/11/18/29257).

## References

- [1] Barbuti A, DiFrancesco D. Control of cardiac rate by "funny" channels in health and disease. *Ann NY Acad Sci* 2008;1123:213-223.
- [2] Chiamvimonvat V, Newman D, et al. A double-blind placebo-controlled evaluation of the human electrophysiologic effects of zatebradine, a sinus node inhibitor. *J Cardiovasc Pharmacol* 1998;32:516-520.
- [3] Verrier RL, Sobrado MF, et al. Inhibition of  $I_f$  in the atrioventricular node as a mechanism for dronedarone's reduction in ventricular rate during atrial fibrillation. *Heart Rhythm* 2013;10:1692-1697.
- [4] Baruscotti M, Bucchi A, et al. Deep bradycardia and heart block caused by inducible cardiac-specific knockout of the pacemaker channel gene *Hcn4*. *PNAS* 2011;108:1705-1710.
- [5] Temple IP, Quigley G, et al. Atrioventricular nodal dysfunction in the monocrotaline rat model of pulmonary arterial hypertension. *Proc Physiol Soc* 2012;28:PC34.
- [6] Inada S, Hancox JC, et al. One-dimensional mathematical model of the atrioventricular node including atrio-nodal, nodal, and nodal-his cells. *Biophys J* 2009;97:2117-2127.
- [7] Liu J, Noble PJ, et al. Role of pacemaking current in cardiac nodes: Insights from a comparative study of sinoatrial node and atrioventricular node. *Prog Biophys Mol Biol.* 2008;96:294-304.
- [8] Lakatta EG, DiFrancesco D. What keeps us ticking: a funny current, a calcium clock, or both? *Journal of Molecular and Cellular Cardiology* 2009;47:157-170.

Address for correspondence.

Jue Li  
 Institute of Cardiovascular Sciences, University of Manchester  
 CTF Building, 46 Grafton Street, Manchester M13 9NT, UK  
 jue.li@manchester.ac.uk